Canadian Journal of
Neurological Sciences

Journal Canadien des
Sciences Neurologiques

Letter to the Editor: New Observation

Management of Giant Anterior Meningocele in a Young Patient with Marfan Syndrome

Vara Giulio[1,2,3] ⬤, Conti Alfredo[4,1], Vornetti Gianfranco[1,5], Gasbarrini Alessandro[1,6], Massimiliano De Paolis[7],

Donti Andrea[7], Mariucci Elisabetta[7], Bombino Alice[1] and Spinardi Luca[7]

[1]University of Bologna, Dipartimento di Scienze Biomediche e Neuromotorie, Università di Bologna, Bologna, Emilia-Romagna, Italy, [2]Casa Di Cura Madre Fortunata Toniolo, Radiology, Bologna, Emilia-Romagna, Italy, [3]Casa di Cura Villa Erbosa, Radiology, Bologna, Emilia-Romagna, Italy, [4]IRCCS Istituto Delle Scienze Neurologiche di Bologna, Neurosurgery Department, Bologna, Emilia-Romagna, Italy, [5]IRCCS Istituto Delle Scienze Neurologiche di Bologna, Functional and Molecular Neuroimaging Unit, Bologna, Emilia-Romagna, Italy, [6]IRCCS Istituto Ortopedico Rizzoli, Spine Surgery Unit, Bologna, Emilia-Romagna, Italy and [7]University of Bologna, IRCCS Azienda Ospedaliero-Universitaria di Bologna, Bologna, Italy

Dural ectasia is a common manifestation of Marfan syndrome, characterized by the progressive weakening and dilation of the dural sac, typically occurring in the lumbar or sacral regions. This condition results from the alteration of connective tissue due to fibrillin-1 deficiency, which compromises the structural integrity of the dura mater. Dural ectasia can cause a range of symptoms, including lower back pain, headaches and neurological deficits, as the expanded dural sac compresses adjacent nerve roots. It is often identified through imaging, with MRI being the modality of choice, showing characteristic ballooning of the dural sac. This condition is particularly relevant in Marfan patients as it may increase the risk of complications such as spinal instability or nerve root compression.[1]

Anterior meningocele, a rare form of spinal dysraphism, occurs when the meninges herniate through a defect in the anterior sacrum, forming a sac that can compress surrounding structures. While this condition is typically congenital, its occurrence in patients affected by Marfan syndrome is exceedingly uncommon.[2] In such cases, anterior meningocele can lead to various complications, including neurological deficits and compression of the urinary tract.

Advanced neuroimaging techniques, such as diffusion tensor imaging (DTI) with tractography, have significantly enhanced the ability to visualize peripheral nerve structures. DTI tractography provides a detailed map of nerve fiber pathways, allowing surgeons to plan interventions while minimizing damage to critical structures.[3] We present the case of a patient with Marfan syndrome who underwent surgical repair of a giant anterior meningocele, in which the use of DTI tractography was pivotal in understanding the relationship between the meningocele and the sacral nerves, guiding the surgical approach.

A 21-year-old female, with a diagnosis of Marfan syndrome since the age of 6, which was confirmed by genetic testing, presented with progressive urinary tract symptoms, including bilateral hydronephrosis. Currarino syndrome was ruled out due to the absence of anorectal and sacral malformations. She is followed up by a cardiologist due to an aortic root dilation with moderate aortic insufficiency, without dilation of the right-sided sections and tricuspid valve insufficiency. She is also under surveillance for scoliosis and wears a spinal orthosis. Her medical history also includes hypertension and tachycardia, for which she is on home therapy with losartan 50 mg daily and bisoprolol 1.25 mg twice daily.

A multiphasic CT scan was ordered to investigate the hydronephrosis better. The findings included bilateral third-degree hydronephrosis; the left ureter showed compression signs caused by a massive anterior meningocele of sacral origin, displacing the pelvic organs. The right kidney was showing initial signs of decreased function, with reduced contrast media excretion, evidenced by a fluid-fluid level in the renal pelvis (Figure 1A–C). Moreover, the renal insufficiency was demonstrated via renal scintigraphy (Supplementary material).

MRI on Insigna® 3T Philips® MRI of the lumbar spine and pelvis was performed, revealing a large anterior meningocele measuring approximately 7 cm in diameter. The meningocele was located in the presacral region, with significant compression of the urinary bladder and surrounding tissues. The routine scanning protocol (sagittal T1-weighted, T2-weighted and STIR sequences and axial T2 sequence) was adjusted with additional sequences, comprising a T2 without flow compensation and shorter TE (Echo Time) to enhance the flow voids, and high-resolution steady-state free precession isotropic sequences to clearly depict the anatomy of the meningocele (Figure 1D–G).

To further assess the relationship between the anterior meningocele and the sacral nerves, DTI with tractography was performed. This advanced imaging modality was crucial in visualizing the course of the sacral nerve roots, especially the S2–S4 nerves, which are primarily responsible for bladder and
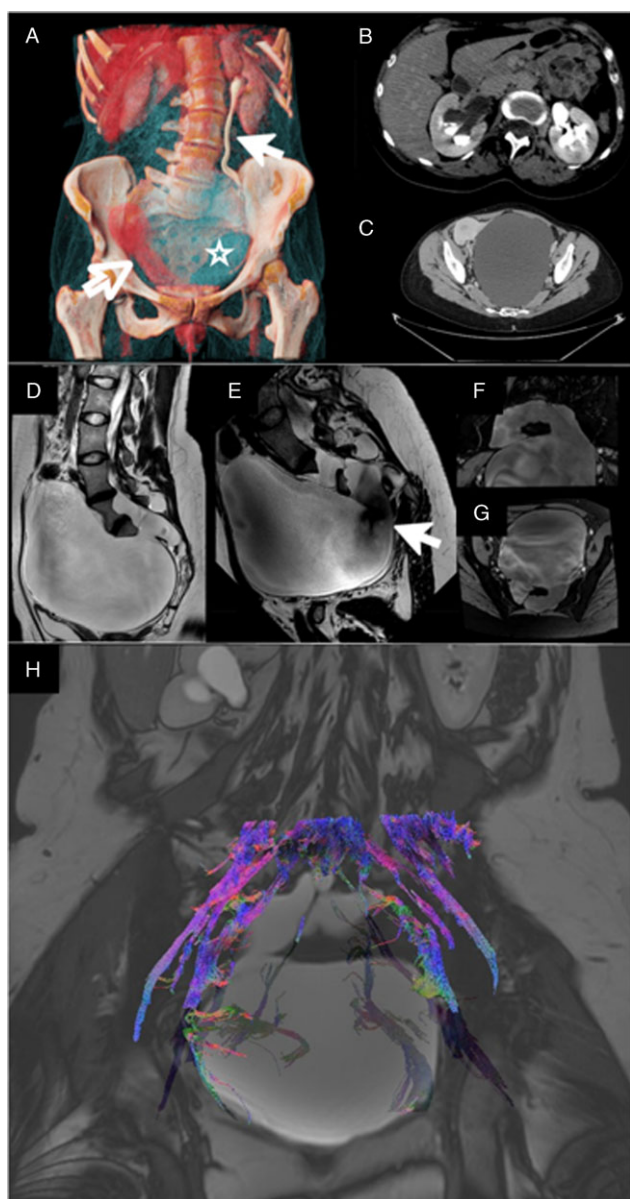
Figure 1. (A) Cinematic rendering of the abdominal CT showing the anterior meningocele (light blue, void star), the displaced uterus (red, void arrow), dilatation of the left ureter (white arrow) and the absence of contrast media elimination from the right kidney. (B) Axial section of the renal pelvis. (C) Axial section of the pelvis. (D) The sagittal T2-weighted sequence shows the extent of the meningocele. (E) Flow-sensitive T2 sequence shows the flow void, highlighting the communication with the spinal canal (void arrow). (F,G) High-resolution steady-state free precession isotropic imaging clearly depicts the anatomy of the communication with the spinal canal, with the possibility to generate multiplanar reconstruction to better plan the surgery. (H) Fiber tracking calculated from diffusion tensorimaging (DTI) superimposed on a low-resolution steady-state sequence. The fibers are color coded for direction: blue for craniocaudal, green for lateral and red for anterior posterior. This image aided the surgeons to avoid nerve roots, especially S2, which was intraoperatively compressed near the foramen.

bowel control. The DTI tractography showed that the nerve fibers were being displaced by the anterior meningocele but remained intact despite the mass effect of the meningeal sac. This finding indicated that surgical decompression would likely result in the resolution of the patient's symptoms without causing nerve injury (Figure 1H).

To perform DTI in this context, specialized diffusion-weighted imaging protocols are used with optimized b-values and gradient directions to capture the anisotropic diffusion in nerves. Post-processing involves reconstructing the nerve pathways using tractography algorithms, which generate three-dimensional maps of nerve trajectories, aiding in surgical planning by differentiating healthy nerves from areas affected by pathology.[4]

For this case, the diffusion data were reconstructed using generalized q-sampling imaging with a diffusion-sampling length ratio of 1.25.[5] Q-sampling imaging was the selected reconstruction method as it does not rely on a specific diffusion model.[6] The anisotropy threshold was 0.011, visually adjusting the threshold to ensure involving only peripheral nerves in the tracking algorithm. The angular threshold was 70 degrees, in agreement with the reported ex vivo studies of the rootlets; this relatively steep angle, compared to the central nervous system's usual thresholds, is helpful when analyzing rootlets for the steep angles in the proximity of the spinal canal.[7]

For the surgery, the patient was placed in a prone position, with the abdomen unloaded and the head supported to allow cranial convexity decompression. A posterior approach was used to first separate the muscles from L4 to the end of the sacrum. Two large automatic retractors were placed, and then laminectomies of L5 and sacral segments (from S1 to S3) were performed. Durotomy from L5 to S3 was performed, and intradural procedures were done under the magnification of the operating exoscope and the use of intraoperative neuromonitoring. The surgical team identified and preserved the posterior sacral roots, in particular the left S2 root, as it was exiting the corresponding neural foramen. The meningocele neck was then identified at this level, giving access to the large anterior cyst. CSF was aspirated at the lumbo-sacral level through the foramina of S2 and S3, which were interconnected. Then, the meningocele neck was ligated with two nonabsorbable threads and cut between the ligatures. An external spinal drainage was inserted for CSF drainage between L4 and L5. The procedure was concluded securing muscular coverage over the sacral dura mater, layered closure and placement of an intermuscular suction drain. Neuromonitoring was not performed during surgery.

Postoperative imaging at different time points (3 and 9 months) shows an excellent therapeutic result, with almost complete collapse of the anterior sacral meningocele walls, currently deflated, with minimal remaining CSF along the anterior left margin of the sacrum (Figure 2C-D-E). There is also an anatomical relocation of the pelvic viscera and minimal residual dilation of the renal pelvis (Figure 2A-B).

This case highlights the rare association of Marfan syndrome with a giant anterior meningocele, leading to urinary tract dysfunction due to compression of the pelvic structures. The use of advanced imaging techniques, particularly DTI with tractography, played a crucial role in the preoperative assessment by providing detailed visualization of the peripheral nervous system, beyond what is achievable with standard morphological imaging alone. DTI tractography enabled the surgical team to accurately map the displaced sacral nerve roots and plan a safe and effective decompression surgery, ultimately resulting in the complete resolution of the patient's urinary symptoms.

This underscores the importance of incorporating advanced neuroimaging into the management of complex cases involving neural structures. By offering a noninvasive method to assess the integrity and spatial relationships of peripheral nerves, DTI provides invaluable information that can guide surgical interventions and improve patient outcomes, especially in conditions like anterior meningocele, where nerve preservation is a primary concern.
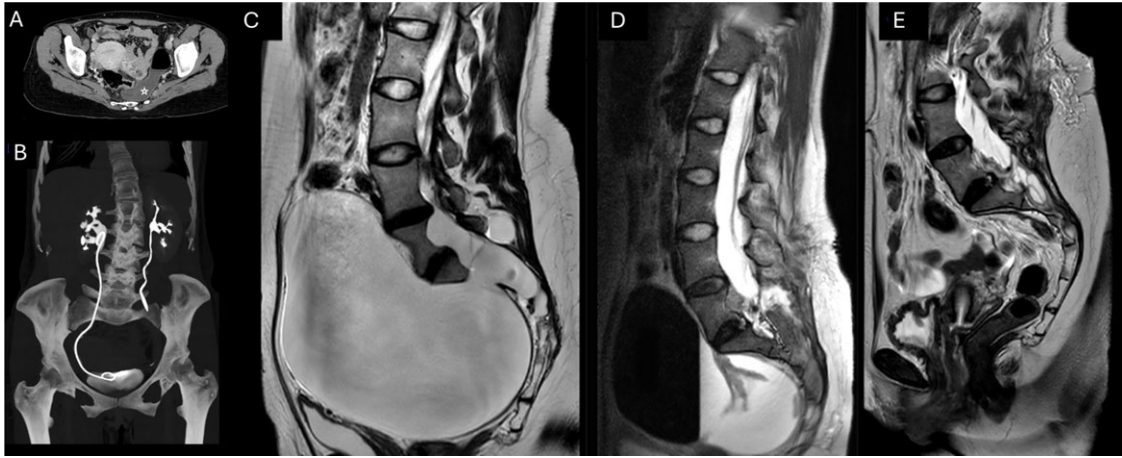
Figure 2. (A) Postoperative CT of the abdomen and pelvis acquired 3 months after surgery. Partial resorption of the meningocele, with air-fluid level, residual in the presacral space (void star), and relocation of the pelvic organs. (B) Coronal maximum intensity projection reconstruction showing partial resolution of the right side hydronephrosis, with a ureteral stent in place, and complete resolution of the dilatation of the left ureter. Sagittal T2-weighted sequences showing the temporal evolution of the meningocele (C) before surgery, (D) after 3 months and (E) after 9 months.

Author contributions. G.Va, G.Vo., L.S.: Writing, study design, imaging studies acquisition, post-processing.

A.G., D.P.M., A.C.: Writing, data collection, surgical management.

A.D., E.M.: Writing, supervision, data collection, clinical management.

A.B.: Writing, proofreading.

Competing interests. None.

Ethical standard. Approval was granted by the local ethical committee (CE–AVEC, reference code: EM624-2019_246/2016/O/Oss/AOUBo), and informed consent was obtained.

References

1. Vornetti G, Vara G, Baroni MC, et al. Quantitative measurement of dural ectasia: associations with clinical and genetic characteristics in Marfan syndrome. *Eur Spine J.* 2024;33:2561–2568. doi: 10.1007/s00586-024-08252-3.

2. Rigante D, Segni G. Anterior sacral meningocele in a patient with Marfan syndrome. *Clin Neuropathol.* 2001;20:70–72.

3. Wolf RL, Nucifora PG, Melhem ER. DTI in neurosurgical planning. In: Van HeckeW, EmsellL, SunaertS, eds. *Diffus Tensor Imaging Pract Handb.* New York, NY, Springer; 2016: pp. 291–308. doi: 10.1007/978-1-4939-3118-7_14.

4. Vara G, Tuzzato G, Bianchi G, et al. Clinical application of diffusion tensor imaging for a brachial plexus injury. *Diagnostics (Basel).* 2022;12(7):1687. doi: 10.3390/diagnostics12071687.

5. Yeh F-C, Wedeen VJ, Tseng W-YI. Generalized q-sampling imaging. *IEEE Trans Med Imaging.* 2010;29:1626–1635. doi: 10.1109/TMI.2010.2045126.

6. Zhang H, Wang Y, Lu T, et al. Differences between generalized q-sampling imaging and diffusion tensor imaging in the preoperative visualization of the nerve fiber tracts within peritumoral edema in brain. *Neurosurgery.* 2013;73:1044–1053. doi: 10.1227/NEU.0000000000000146. discussion 1053.

7. Henssen DJHA, Weber RC, de Boef J, et al. Post-mortem 11.7 Tesla magnetic resonance imaging vs. polarized light imaging microscopy to measure the angle and orientation of dorsal root afferents in the human cervical dorsal root entry zone. *Front Neuroanat.* 2019;13:66. doi: 10.3389/fnana.2019.00066.